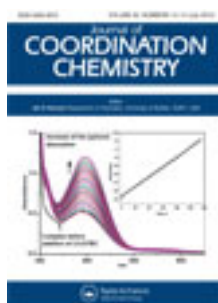


This article was downloaded by: [Renmin University of China]

On: 13 October 2013, At: 10:35

Publisher: Taylor & Francis

Informa Ltd Registered in England and Wales Registered Number: 1072954 Registered office: Mortimer House, 37-41 Mortimer Street, London W1T 3JH, UK



Journal of Coordination Chemistry

Publication details, including instructions for authors and subscription information:

<http://www.tandfonline.com/loi/gcoo20>

2-Aminobenzothiazole-based Cd^{II} complexes incorporating carboxylate-containing coligand: synthesis, crystal structure, and fluorescences

Xiu-Guang Wang^a, En-Chan Wang^a, Jian Li^a, Xiao-Jun Zhao^a & En-Cui Yang^a

^a College of Chemistry, Tianjin Key Laboratory of Structure and Performance for Functional Molecules, Tianjin Normal University, Tianjin 300387, P. R. China

Accepted author version posted online: 09 May 2012. Published online: 31 May 2012.

To cite this article: Xiu-Guang Wang, En-Chan Wang, Jian Li, Xiao-Jun Zhao & En-Cui Yang (2012) 2-Aminobenzothiazole-based Cd^{II} complexes incorporating carboxylate-containing coligand: synthesis, crystal structure, and fluorescences, Journal of Coordination Chemistry, 65:13, 2353-2364, DOI: [10.1080/00958972.2012.692471](https://doi.org/10.1080/00958972.2012.692471)

To link to this article: <http://dx.doi.org/10.1080/00958972.2012.692471>

PLEASE SCROLL DOWN FOR ARTICLE

Taylor & Francis makes every effort to ensure the accuracy of all the information (the "Content") contained in the publications on our platform. However, Taylor & Francis, our agents, and our licensors make no representations or warranties whatsoever as to the accuracy, completeness, or suitability for any purpose of the Content. Any opinions and views expressed in this publication are the opinions and views of the authors, and are not the views of or endorsed by Taylor & Francis. The accuracy of the Content should not be relied upon and should be independently verified with primary sources of information. Taylor and Francis shall not be liable for any losses, actions, claims, proceedings, demands, costs, expenses, damages, and other liabilities whatsoever or howsoever caused arising directly or indirectly in connection with, in relation to or arising out of the use of the Content.

This article may be used for research, teaching, and private study purposes. Any substantial or systematic reproduction, redistribution, reselling, loan, sub-licensing, systematic supply, or distribution in any form to anyone is expressly forbidden. Terms &

Conditions of access and use can be found at <http://www.tandfonline.com/page/terms-and-conditions>

2-Aminobenzothiazole-based Cd^{II} complexes incorporating carboxylate-containing coligand: synthesis, crystal structure, and fluorescences

XIU-GUANG WANG, EN-CHAN WANG, JIAN LI,
XIAO-JUN ZHAO and EN-CUI YANG*

College of Chemistry, Tianjin Key Laboratory of Structure and Performance for Functional Molecules, Tianjin Normal University, Tianjin 300387, P. R. China

(Received 25 November 2011; in final form 28 March 2012)

Four new 2-aminobenzothiazole (abt)-based Cd^{II} complexes, {[Cd(abt)₂(chdc)][Cd(abt)₂(chdc)]·2H₂O·CH₃OH}_n (**1**), [Cd₂(abt)₄(bd)(H₂O)₂]·2H₂O (**2**), [Cd(abt)₂(*o*-mb)₂] (**3**), and [Cd(abt)₂(*m*-mb)₂] (**4**) (chdc = *cis*-1,4-cyclohexanedicarboxylate, bd = *cis*-butenedicarboxylate, *o*-mb = *o*-methylbenzoate, and *m*-mb = *m*-methylbenzoate), were obtained by the reaction of Cd^{II} with abt ligand in the presence of different carboxylate-containing coligands. As a result of the different number of carboxylate groups appended on the coligands, the complexes exhibit H-bonded supramolecular assemblies consisting of polymeric 1-D array and separate binuclear entity for **1**, a centrosymmetric binuclear structure for **2** as well as discrete mononuclear entities for **3** and **4**, which are further packed into 2-D supramolecular networks by hydrogen-bonding and/or π - π stacking interactions. The four complexes with comparable thermal stability display intense abt-based emissions, suggesting their potential applications as fluorescent materials.

Keywords: 2-Aminobenzothiazole; Crystal structure; Thermal stability; Fluorescent

1. Introduction

Crystal engineering involving metal ions and organic ligands has attracted considerable attention because of intriguing topologies [1] and promising applications in magnetism, electricity, and gas sorption [2]. In contrast to the binding preferences of metal ions, the nature of organic ligands including the type, number, and the position of the binding group, the electronic structure, as well as the steric tension of the ligand skeleton may play important roles on the overall framework connectivity and physical/chemical performance. Intermolecular weak interactions such as hydrogen bonding and π - π stacking can also help to tailor the higher-dimensional networks of the resulting target complexes [3]. Benzothiazole and derivatives have been examined for their strong heterocyclic N donor to coordinate to metal ion as well as their benzothiazole-derived biological and optical activities in medicine, agriculture, and molecular devices [4–8].

*Corresponding author. Email: encui_yang@yahoo.com.cn

As continuation of our interest in structures and fluorescent properties of mixed ligand metal complexes [6, 9, 10], in the present contribution, 2-aminobenzothiazole (abt) was selected as a ligand to react with Cd^{II} and various carboxylate-containing organic acids such as *cis*-1,4-cyclohexanedicarboxylic acid (H_2chdc), *cis*-butenedicarboxylic acid (H_2bd), *o*-methylbenzoic acid (*o*-Hmb), and *m*-methylbenzoic acid (*m*-Hmb). Herein, we investigate the influences of the number/position of the carboxylate as well as the skeletal nature of the coligands on the abt-based ternary system. As a result, four Cd^{II} -containing complexes with combined polymeric chain and centrosymmetric binuclear motif for **1**, centrosymmetric binuclear entity for **2**, and discrete mononuclear structures for **3** and **4** were isolated and characterized. Due to the same binding modes adopted by bidentate chelating carboxylate group and terminal monodentate abt, the structural diversity of **1–4** is dominated by the number of carboxylates and the backbone flexibility of the organic coligands. The thermal stability and the fluorescent emission of the four complexes were also investigated.

2. Experimental

2.1. Reagents and instruments

Commercially available chemicals were used without purification abt was purchased from Acros and other analytical-grade reagents were from Tianjin Chemical Reagent Factory. Doubly deionized water was used for synthesis. Elemental analyses (C, H, and N) were carried out with a CE-440 (Leeman-Labs) analyzer. Fourier transform (FT) Infrared (IR) spectra (KBr pellets) were taken on an Avatar-370 (Nicolet) spectrometer from 4000 to 400 cm^{-1} . Thermogravimetric analysis experiments were carried out on a Shimadzu simultaneous DTG-60 A compositional analysis instrument from room temperature to 800°C under N_2 at a heating rate of 5°C min^{-1} . Fluorescence spectra of polycrystalline powder samples were performed on a Cary Eclipse fluorescence spectrophotometer (Varian) equipped with a xenon lamp and quartz carrier at room temperature.

2.2. Synthesis of $\{[\text{Cd}(\text{abt})_2(\text{chd})][\text{Cd}(\text{abt})_2(\text{chd})]\cdot 2\text{H}_2\text{O}\cdot \text{CH}_3\text{OH}\}_n$ (**1**)

To a methanol solution (10.0 mL) containing abt (30.0 mg, 0.2 mmol) and H_2chdc (17.2 mg, 0.1 mmol), an aqueous solution (5.0 mL) of $\text{Cd}(\text{OAc})_2\cdot 2\text{H}_2\text{O}$ (26.6 mg, 0.1 mmol) was slowly added with constant stirring. The resulting mixture was further stirred for 1 h and filtered. Colorless block-shaped crystals suitable for X-ray diffraction were obtained by slow evaporation of the filtrate for 7 days (yield: 65% based on Cd^{II} salt). Anal. Calcd for $\text{C}_{45}\text{H}_{52}\text{Cd}_2\text{N}_8\text{O}_{11}\text{S}_4$ (%): C, 43.80; H, 4.25; N, 9.08. Found (%): C, 43.84; H, 4.27; N, 9.10. IR (KBr, cm^{-1}): 3311 m, 3166 m, 2938 m, 1635 w, 1536 s, 1431 m, 1329 w, 919 w, 745 m, and 583 w.

2.3. Synthesis of $\{[\text{Cd}(\text{abt})_2(\text{bd})(\text{H}_2\text{O})]_2\cdot 2\text{H}_2\text{O}\}$ (**2**)

Similar synthetic procedures as those of **1** were employed for **2** except that H_2chdc and $\text{Cd}(\text{OAc})_2\cdot 2\text{H}_2\text{O}$ were replaced by H_2bd (11.6 mg, 0.1 mmol) and $\text{Cd}(\text{NO}_3)_2\cdot 4\text{H}_2\text{O}$

(30.8 mg, 0.1 mmol). Colorless block-shaped crystals suitable for X-ray diffraction were obtained within 1 week (yield: 40% based on Cd^{II} salt). Anal. Calcd for C₁₈H₁₈CdN₄O₆S₂ (%): C, 38.40; H, 3.22; N, 9.95. Found (%): C, 38.42; H, 3.20; N, 9.98. IR (KBr, cm⁻¹): 3301 m, 3330 m, 3137 m, 1650 m, 1549 vs, 1455 s, 1412 w, 1343 w, 1312 m, 1289 m, 1251 m, 1131 w, 1020 w, 895 w, 862 m, 749 s, 721 m, 702 w, and 659 w.

2.4. Synthesis of [Cd(abt)₂(*o*-mb)₂] (3) and [Cd(abt)₂(*m*-mb)₂] (4)

The preparation procedures of **3** and **4** were similar to **1**, except that H₂chdc was replaced by *o*-Hmb and *m*-Hmb (13.6 mg, 0.1 mmol), respectively. Yield: 62% for **3** and 49% for **4** based on Cd^{II} salt. Anal. Calcd for C₃₀H₂₆CdN₄O₄S₂ (**3**) (%): C, 52.75; H, 3.84; N, 8.20. Found (%): C, 52.71; H, 3.91; N, 8.16. IR (KBr, cm⁻¹): 3319 s, 3154 m, 1630 w, 1523 vs, 1409 s, 1142 w, 869 w, 739 m, and 542 m. Anal. Calcd for C₃₀H₂₆CdN₄O₄S₂ (**4**) (%): C, 52.75; H, 3.84; N, 8.20. Found (%): C, 52.71; H, 3.81; N, 8.16. IR (KBr, cm⁻¹): 3341 s, 3189 m, 1633 w, 1528 vs, 1405 s, 750 m, and 518 m.

2.5. X-ray crystallography

Diffraction intensities for **1–4** were collected on a Bruker APEX-II CCD diffractometer at ambient temperature with Mo-K α radiation ($\lambda = 0.71073 \text{ \AA}$) using the φ - ω scan mode. Semiempirical multi-scan absorption corrections were applied using SADABS and the program SAINT was used for integration of the diffraction profiles. The structures were solved by direct methods using SHELXS of the SHELXTL package and refined with SHELXL [11, 12]. The final refinement was performed by full-matrix least-squares on F^2 with anisotropic thermal parameters for all non-hydrogen atoms. The positions of hydrogen atoms bonded to carbon were generated geometrically and allowed to ride on their parent carbons before the final cycle of refinement. Hydrogen atoms attached to oxygen were first located in difference Fourier maps and then placed in calculated sites, and refined isotropically. The crystallographic data and selected bond lengths and angles for **1–4** are listed in tables 1–5. Hydrogen-bonding parameters are summarized in table 6.

3. Results and discussion

3.1. Syntheses and FT-IR spectra

Complexes **1–4** were prepared by introducing different coligands under conventional room-temperature evaporation method. In IR spectra, a weak band at 3311 cm⁻¹ for **1**, 3301 cm⁻¹ for **2**, 3319 cm⁻¹ for **3**, and 3341 cm⁻¹ for **4** are ascribed to the stretch of the exocyclic amino group of abt [6]. The absence of a strong absorption at 1700 cm⁻¹ indicates full deprotonation of the carboxylic group in **1–4** [13]. The characteristic bands for the asymmetric and symmetric stretching vibrations of the carboxylate were observed at 1600–1400 cm⁻¹. Upon cation binding, the characteristic band for C=N of abt shifts from 1527 cm⁻¹ in free abt to 1536, 1549, 1523, and 1528 cm⁻¹ for

Table 1. Crystal data and structure refinement for 1–4.

	1	2	3	4
Empirical formula	C ₄₅ H ₅₂ Cd ₂ N ₈ O ₁₁ S ₄	C ₁₈ H ₁₈ CdN ₄ O ₈ S ₂	C ₃₀ H ₃₀ CdN ₄ O ₄ S ₂	C ₃₀ H ₂₆ CdN ₄ O ₄ S ₂
Formula weight (g mol ⁻¹)	1233.99	562.88	683.07	683.07
Crystal system	Monoclinic	Monoclinic	Monoclinic	Monoclinic
Space group	<i>P</i> 2 ₁ / <i>c</i>	<i>C</i> 2/ <i>c</i>	<i>P</i> 2 ₁ / <i>n</i>	<i>C</i> 2/ <i>c</i>
Unit cell dimensions (Å, °)				
<i>a</i>	9.7644(14)	34.704(5)	10.3466(5)	23.3411(15)
<i>b</i>	29.983(5)	8.5341(13)	11.3565(6)	12.8795(8)
<i>c</i>	18.791(3)	15.904(3)	25.0991(12)	19.9613(13)
β	100.655(2)	107.032(2)	94.0920(10)	96.8040(10)
Volume (Å ³), <i>Z</i>	5406.6(14), 4	4503.7(12), 8	2941.7(3), 4	5958.5(7), 8
Calculated density (g cm ⁻³)	1.516	1.660	1.542	1.523
Absorption coefficient (mm ⁻¹)	1.003	1.196	0.927	0.915
<i>F</i> (000)	2504	2256	1384	2768
Crystal size (mm ³)	0.25 × 0.23 × 0.21	0.21 × 0.19 × 0.14	0.25 × 0.23 × 0.22	0.20 × 0.18 × 0.15
Limiting indices	-10 ≤ <i>h</i> ≤ 11; -35 ≤ <i>k</i> ≤ 32; -22 ≤ <i>l</i> ≤ 21	-41 ≤ <i>h</i> ≤ 39; -9 ≤ <i>k</i> ≤ 10; -18 ≤ <i>l</i> ≤ 18	-12 ≤ <i>h</i> ≤ 12; -12 ≤ <i>k</i> ≤ 13; -28 ≤ <i>l</i> ≤ 29	-26 ≤ <i>h</i> ≤ 27; -15 ≤ <i>k</i> ≤ 12; -23 ≤ <i>l</i> ≤ 23
Reflections collected	29,274	11,815	15,728	15,923
Independent reflection	9529 [<i>R</i> (int) = 0.0463]	3938 [<i>R</i> (int) = 0.0347]	5181 [<i>R</i> (int) = 0.0171]	5255 [<i>R</i> (int) = 0.0359]
Max. and min. transmission	0.8171 and 0.7877	0.8504 and 0.7872	0.8221 and 0.8014	0.8526 and 0.8103
Data/restraints/parameters	9529/0/631	3938/0/280	5181/0/372	5255/0/372
Goodness-of-fit on <i>F</i> ²	1.025	1.019	1.033	1.013
Final <i>R</i> indices [<i>I</i> > 2σ(<i>I</i>)] ^a	<i>R</i> ₁ = 0.0381, <i>wR</i> ₂ = 0.0830	<i>R</i> ₁ = 0.0314, <i>wR</i> ₂ = 0.0741	<i>R</i> ₁ = 0.0209, <i>wR</i> ₂ = 0.0513	<i>R</i> ₁ = 0.0339, <i>wR</i> ₂ = 0.0706
<i>R</i> indices (all data)	<i>R</i> ₁ = 0.0698, <i>wR</i> ₂ = 0.0933	<i>R</i> ₁ = 0.0478, <i>wR</i> ₂ = 0.0808	<i>R</i> ₁ = 0.0263, <i>wR</i> ₂ = 0.0531	<i>R</i> ₁ = 0.0607, <i>wR</i> ₂ = 0.0794
Largest difference peak and hole (e Å ⁻³)	0.607 and -0.434	0.593 and -0.448	0.216 and -0.263	0.275 and -0.298

^a*R*₁ = Σ(|*F*_o - |*F*_c||) / Σ|*F*_o|; *wR*₂ = [Σw(|*F*_o|² - |*F*_c|²)² / Σw(*F*_o)²]^{1/2}.

Table 2. Selected bond lengths (Å) and angles (°) for 1.

Cd(1)–N(3)	2.271(4)	Cd(1)–N(1)	2.282(3)
Cd(1)–O(3) ^a	2.310(3)	Cd(1)–O(1)	2.352(3)
Cd(1)–O(2)	2.361(3)	Cd(1)–O(4) ^a	2.419(3)
Cd(2)–N(5)	2.271(3)	Cd(2)–O(5)	2.307(3)
Cd(2)–O(7) ^b	2.308(3)	Cd(2)–N(7)	2.320(3)
Cd(2)–O(6)	2.428(3)	Cd(2)–O(8) ^b	2.453(3)
N(3)–Cd(1)–N(1)	90.65(13)	N(3)–Cd(1)–O(3) ^a	117.26(13)
N(1)–Cd(1)–O(3) ^a	96.18(12)	N(3)–Cd(1)–O(1)	96.43(13)
N(1)–Cd(1)–O(1)	121.22(13)	O(3) ^a –Cd(1)–O(1)	129.56(13)
N(3)–Cd(1)–O(2)	146.74(13)	N(1)–Cd(1)–O(2)	92.50(12)
O(3) ^a –Cd(1)–O(2)	95.30(12)	O(1)–Cd(1)–O(2)	54.29(11)
N(3)–Cd(1)–O(4) ^a	85.47(13)	N(1)–Cd(1)–O(4) ^a	143.39(11)
O(3) ^a –Cd(1)–O(4) ^a	54.79(11)	O(1)–Cd(1)–O(4) ^a	95.39(13)
N(5)–Cd(2)–O(5)	119.72(13)	N(5)–Cd(2)–O(7) ^b	145.66(12)
O(5)–Cd(2)–O(7) ^b	93.75(12)	N(5)–Cd(2)–N(7)	92.62(12)
O(5)–Cd(2)–N(7)	87.94(12)	O(7) ^b –Cd(2)–N(7)	96.27(12)
N(5)–Cd(2)–O(6)	104.67(11)	O(5)–Cd(2)–O(6)	55.00(10)
O(7) ^b –Cd(2)–O(6)	87.67(11)	N(7)–Cd(2)–O(6)	142.93(11)
N(5)–Cd(2)–O(8) ^b	92.24(12)	O(5)–Cd(2)–O(8) ^b	140.76(11)
O(7) ^b –Cd(2)–O(8) ^b	53.98(11)	N(7)–Cd(2)–O(8) ^b	114.53(13)
O(6)–Cd(2)–O(8) ^b	97.56(12)		

Symmetry codes: ^a $x, 3/2 - y, z + 1/2$; ^b $1 - x, 1 - y, 1 - z$.

Table 3. Selected bond lengths (Å) and angles (°) for 2.

Cd(1)–N(3)	2.304(3)	Cd(1)–N(1)	2.314(3)
Cd(1)–O(3) ^a	2.327(3)	Cd(1)–O(5)	2.379(2)
Cd(1)–O(1)	2.381(3)	Cd(1)–O(2)	2.577(3)
Cd(1)–O(4) ^a	2.594(3)		
N(3)–Cd(1)–N(1)	97.26(10)	N(3)–Cd(1)–O(3) ^a	88.29(10)
N(1)–Cd(1)–O(3) ^a	140.05(10)	N(3)–Cd(1)–O(5)	168.72(9)
N(1)–Cd(1)–O(5)	88.81(9)	O(3) ^a –Cd(1)–O(5)	81.00(8)
N(3)–Cd(1)–O(1)	104.93(10)	N(1)–Cd(1)–O(1)	89.16(10)
O(3) ^a –Cd(1)–O(1)	127.65(9)	O(5)–Cd(1)–O(1)	84.58(9)
N(3)–Cd(1)–O(2)	96.61(10)	N(1)–Cd(1)–O(2)	140.95(9)
O(3) ^a –Cd(1)–O(2)	76.60(8)	O(5)–Cd(1)–O(2)	84.40(9)
O(1)–Cd(1)–O(2)	51.97(8)	N(3)–Cd(1)–O(4) ^a	97.44(9)
N(1)–Cd(1)–O(4) ^a	87.55(9)	O(3) ^a –Cd(1)–O(4) ^a	52.51(8)
O(5)–Cd(1)–O(4) ^a	73.24(8)	O(1)–Cd(1)–O(4) ^a	157.63(9)
O(2)–Cd(1)–O(4) ^a	126.39(8)		

Symmetry codes: ^a $-x, 1 - y, -z$.

Table 4. Selected bond lengths (Å) and angles (°) for 3.

Cd(1)–N(1)	2.2523(16)	Cd(1)–O(2)	2.2895(14)
Cd(1)–N(3)	2.2985(16)	Cd(1)–O(4)	2.3060(15)
Cd(1)–O(3)	2.4107(14)	Cd(1)–O(1)	2.4597(15)
N(1)–Cd(1)–O(2)	108.56(6)	N(1)–Cd(1)–N(3)	100.58(6)
O(2)–Cd(1)–N(3)	93.18(5)	N(1)–Cd(1)–O(4)	95.41(6)
O(2)–Cd(1)–O(4)	146.31(5)	N(3)–Cd(1)–O(4)	105.59(5)
N(1)–Cd(1)–O(3)	150.44(6)	O(2)–Cd(1)–O(3)	98.85(5)
N(3)–Cd(1)–O(3)	88.46(5)	O(4)–Cd(1)–O(3)	55.04(5)
N(1)–Cd(1)–O(1)	100.07(6)	O(2)–Cd(1)–O(1)	54.76(5)
N(3)–Cd(1)–O(1)	146.18(5)	O(4)–Cd(1)–O(1)	98.79(5)
O(3)–Cd(1)–O(1)	86.61(5)		

Table 5. Selected bond lengths (Å) and angles (°) for **4**.

Cd(1)–O(2)	2.277(2)	Cd(1)–N(1)	2.285(3)
Cd(1)–N(3)	2.292(3)	Cd(1)–O(3)	2.310(2)
Cd(1)–O(4)	2.403(3)	Cd(1)–O(1)	2.485(3)
O(2)–Cd(1)–N(1)	114.80(10)	O(2)–Cd(1)–N(3)	93.05(10)
N(1)–Cd(1)–N(3)	91.66(10)	O(2)–Cd(1)–O(3)	140.17(9)
N(1)–Cd(1)–O(3)	92.95(10)	N(3)–Cd(1)–O(3)	115.15(10)
O(2)–Cd(1)–O(4)	93.62(9)	N(1)–Cd(1)–O(4)	147.92(10)
N(3)–Cd(1)–O(4)	101.83(10)	O(3)–Cd(1)–O(4)	54.96(9)
O(2)–Cd(1)–O(1)	54.42(9)	N(1)–Cd(1)–O(1)	93.02(9)
N(3)–Cd(1)–O(1)	145.70(10)	O(3)–Cd(1)–O(1)	98.52(9)
O(4)–Cd(1)–O(1)	91.86(9)		

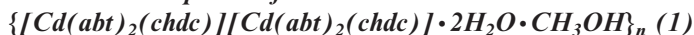
Table 6. Hydrogen-bonding parameters (Å, °) for **1–4**.

Donor –H...Acceptor	<i>d</i> (D–H)	<i>d</i> (H...A)	<i>d</i> (D...A)	∠DHA
1				
N6–H6B...O4 ^a	0.86	2.106	2.953(2)	168
N8–H8B...O2 ^b	0.86	2.019	2.872(9)	172
N2–H2B...O11 ^a	0.86	1.914	2.758(7)	167
O11–H11A...O7	0.85	2.017	2.864(4)	174
2				
O6–H6B...O3 ^a	0.85	1.899	2.706(9)	158
N2–H2B...O6 ^b	0.86	2.024	2.833(3)	156
N4–H4B...O4 ^c	0.86	1.966	2.800(4)	163
O6–H6A...O1 ^d	0.85	1.912	2.742(5)	165
O5–H5B...O6 ^e	0.85	1.925	2.732(7)	158
3				
N2–H2B...O1 ^a	0.86	2.050	2.880(9)	162
N4–H4B...O3 ^b	0.86	2.027	2.860(5)	163
4				
N2–H2B...O1 ^a	0.86	2.092	2.845(7)	146
N4–H4B...O4 ^b	0.86	2.092	2.868(2)	150

Symmetry codes for **1**: ^a $x, 3/2 - y, z + 1/2$; ^b $1 - x, y - 1/2, 3/2 - z$; for **2**: ^a $-x, 1 - y, -z$; ^b $x, 1 - y, z - 1/2$; ^c $-x, y, 1/2 - z$; ^d $x, y - 1, z$; ^e $-x, 1 - y, -z$; for **3**: ^a $1/2 - x, y + 1/2, 1/2 - z$; ^b $-x, -y, -z$; for **4**: ^a $3/2 - x, 1/2 - y, 2 - z$; ^b $2 - x, -y, 2 - z$.

1–4, respectively. Thus, the IR spectra are in agreement with crystal structure determinations.

3.2. Structure descriptions of



Complex **1** crystallizing in monoclinic $P2_1/c$ space group exhibits an H-bonded supramolecular assembly consisting of a discrete centrosymmetrically binuclear structure and a deprotonated chdc-bridged polymeric chain. The asymmetric unit of **1** contains two unique Cd^{II} ions, four neutral abt, two doubly deprotonated chdc, two lattice water molecules, and one free methanol. As shown in figure 1(a), both the crystallographically independent Cd^{II} ions are in distorted octahedral coordination

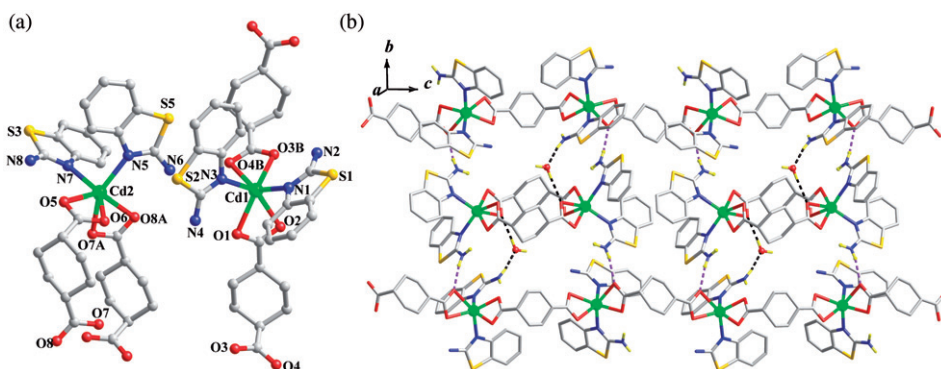


Figure 1. (a) Local coordination environment of Cd^{II} in **1** (hydrogen atoms are omitted for clarity; symmetry codes for A = 1 - x, 1 - y, 1 - z; B = x, 1.5 - y, z + 0.5). (b) 2-D supramolecular layer of **1** formed by hydrogen-bonding interactions.

geometries formed by four chelating carboxylate O donors coming from two separate chdc ligands, and two thiazole nitrogen atoms belonging to two neutral abt ligands. The Cd–O and Cd–N separations are 2.271–2.453 Å, comparable to those typical values [10].

One deprotonated chdc adopts a bis-bidentate chelating mode to link adjacent Cd1 ions into a chain along the crystallographic *c*-axis with the nearest Cd^{II}...Cd^{II} separation of 9.4102(14) Å (figure 1b). In contrast, the other unique chdc dianion in **1** aggregates two centrosymmetric Cd2 ions into a discrete binuclear structure also in a bis-bidentate chelating mode. The intermetallic separation in the binuclear entity (8.2511(12) Å) is slightly shorter than that in the chain. The cyclohexane of both chdc ligands is in a chair-conformation.

In the packing structure of **1**, individual binuclear units are connected with the polymeric chain through N–H...O and O–H...O hydrogen-bonding interactions between the free amino group of abt and the deprotonated carboxylate of chdc. As both donor and acceptor of the hydrogen-bonding interaction, lattice water molecule in **1** is trapped into the 2-D supramolecular network by two-fold O–H...O and N–H...O non-covalent interactions (figure 1b and table 6).

3.3. Structure descriptions of [Cd₂(abt)₄(bd)₂(H₂O)₂]·2H₂O (**2**)

Different from **1**, compound **2** has a centrosymmetric binuclear entity aggregated by a pair of symmetry-related bis-bidentate chelating bd coligand. The asymmetric unit of **2** contains a Cd^{II}, two neutral abt, one fully deprotonated bd, a bound, and a lattice water molecule. As shown in figure 2(a), the sole Cd^{II} in **2** is seven-coordinate to four bidentate chelating carboxylate oxygen atoms from two bd, two terminal thiazole N donors from two abt, and one coordinated water molecule. The coordination geometry around Cd^{II} is an irregular pentagonal bipyramid, in which Cd^{II} deviates from the least-square plane generated by O1–O2–O3A–O4A–N1 only 0.3132 Å. The Cd–N and Cd–O bond lengths range from 2.304(3) to 2.594(3) Å (table 2), comparable with the typical values [6].

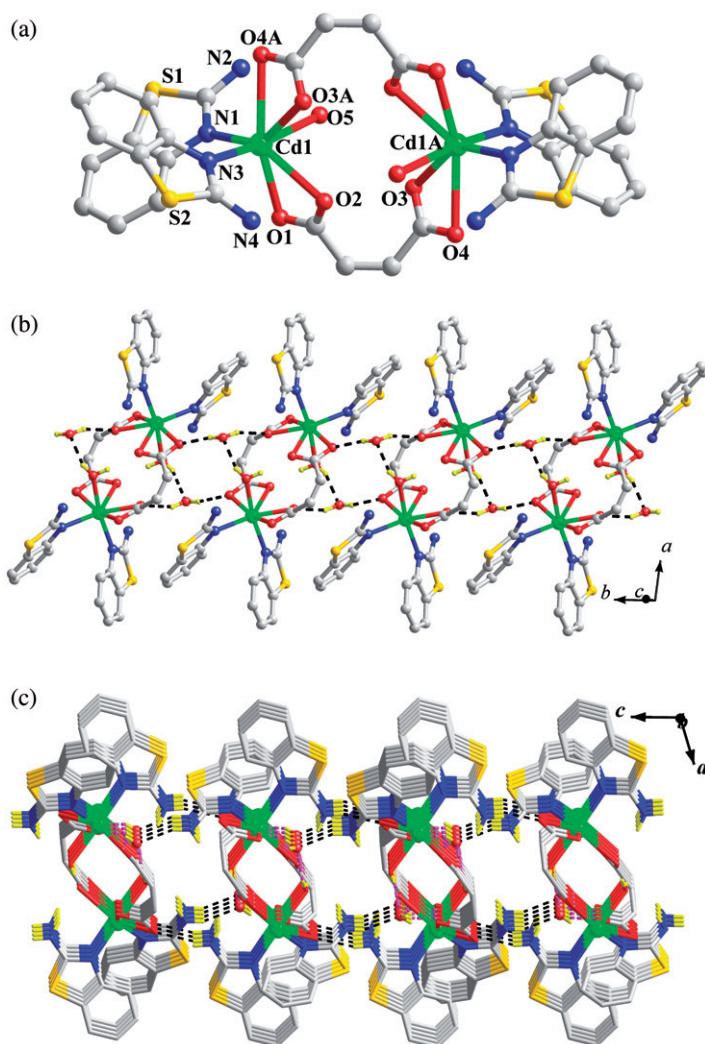


Figure 2. (a) Binuclear entity of **2** (hydrogen atoms are omitted for clarity; symmetry codes for A = $-x, 1 - y, -z$). (b) 2-D layer of **2** by intermolecular N-H \cdots O and O-H \cdots O hydrogen-bonding interactions. (c) 3-D supramolecular connectivity of **2** by non-covalent N-H \cdots O interactions.

Two centrosymmetric bd anions hold two adjacent Cd^{II} ions in a bis-bidentate chelating fashion to generate a binuclear structure of **2** with Cd^{II} \cdots Cd^{II} separation of 5.68537 Å. The intermetallic distance in **2** is comparable with dimeric Cu^{II}-complexes with the same mixed ligands [8].

Behaving as both donor and acceptor, lattice water molecules in **2** connect the separate binuclear units into an infinite 1-D chain through O-H \cdots O and N-H \cdots O hydrogen-bonding interactions produced by the carboxylate group of bd and the amino group of abt (table 6 and figure 2b). As shown in figure 2(c), the 1-D chains are H-bonded together by two-fold N-H \cdots O hydrogen-bonding interactions between the amino group of abt ligand and lattice water molecule/carboxylate of bd (table 6), generating a 3-D supramolecular network of **2**.

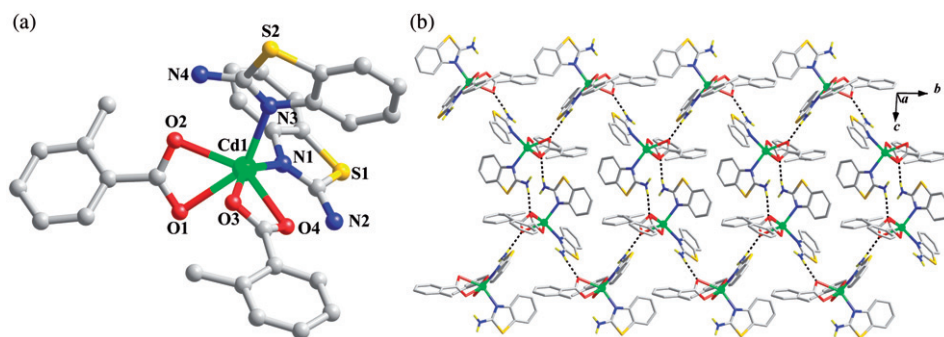


Figure 3. (a) Mononuclear structure of **3**. (b) 2-D supramolecular network of **3** formed by N-H...O hydrogen-bonding interactions.

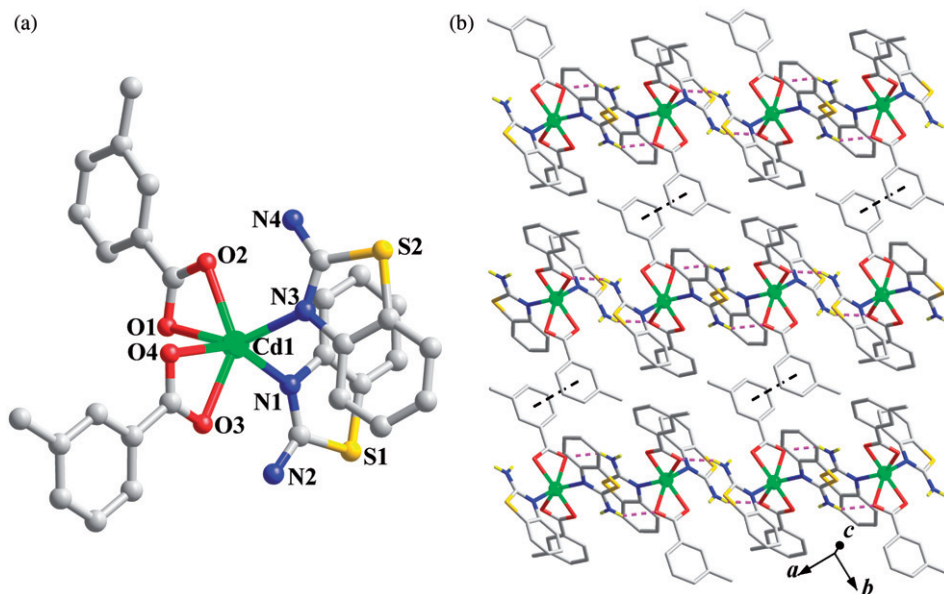


Figure 4. (a) Mononuclear entity of **4**. (b) 2-D supramolecular network of **4** formed by N-H...O hydrogen-bonding and $\pi \cdots \pi$ interactions.

3.4. Structure descriptions of $[Cd(abt)_2(o-mb)_2]$ (**3**) and $[Cd(abt)_2(m-mb)_2]$ (**4**)

Despite the positional isomerism of the carboxylate, both **3** and **4** exhibit discrete mononuclear structures, crystallizing from the same monoclinic crystal system but different space groups ($P2_1/n$ for **3** and $C2/c$ for **4**, table 1). As shown in figures 3(a) and 4(a), the coordination polyhedron around Cd^{II} in **3** and **4** can be described as a distorted octahedron defined by four bidentate-chelating carboxylate oxygen atoms from two separate *o*-/*m*-mb molecules and two thiazole donors from two different abt ligands. The NO₃ donors from a terminal abt ligand and two *o*-/*m*-mb coligands occupy the equatorial plane of Cd1, and the other terminally coordinated abt and one

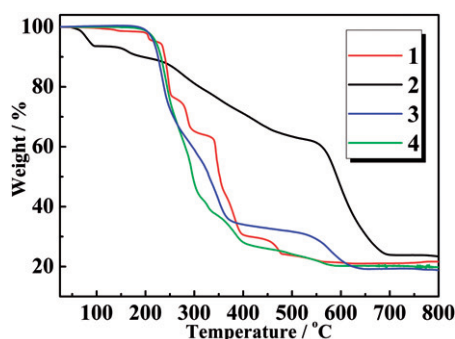


Figure 5. TG curves for 1–4.

carboxylate from *o*-/*m*-mb anion are in the axial positions of the octahedral Cd^{II}. The Cd–O and Cd–N bond lengths fall in the normal ranges (tables 4 and 5). Similar to **1** and **2**, the two crystallographically unique abt ligands in **3** and **4** are unidentate with Cd^{II} via the thiazole nitrogen. The individual mononuclear entities in **3** are arranged into a 2-D planar layer by two-fold non-covalent N–H···O hydrogen bonds between amino of abt and carboxylate of *o*-mb (figure 3b and table 6).

Similar to **3**, the discrete mononuclear entities of **4** are arranged into 1-D chains through two kinds of N–H···O hydrogen bonds from amino of abt and carboxylate of *m*-mb anion (table 6 and figure 4b). Much different from the hydrogen-bonding interactions of **3**, these 1-D chains of **4** are further packed by π – π stacking interactions between parallel benzene rings from two neighboring chains to fabricate a 2-D supramolecular network. The centroid-to-centroid distance and the dihedral angle of the two benzothiazole rings are 3.796 Å and 180°, respectively.

3.5. Thermal stability

TG measurements were carried out to explore the thermal stability of **1–4** (figure 5). Compounds **1** and **2** exhibit two weight-loss stages because of the presence of lattice molecules. The first stage of **1** was from room temperature to 210°C, corresponding to the removal of lattice water molecule and methanol (Expt: 4.9%, Calcd: 5.5%). The synchronous loss of organic ligands in **1** occurred between 230°C and 574°C. The coordinated and lattice water molecules in **2** were removed between 60°C and 93°C (Expt: 6.4%, Calcd: 6.4%); the next obvious weight-loss began at 120°C and ended at 704°C, ascribed to synchronous decomposition of abt and bd. Compounds **3** and **4** display only one weight-loss process corresponding to the decomposition of the ligands from 190°C to 638°C for **3** and between 190°C and 576°C for **4**. The final product of the complexes was CdO (Obsd: 21.0%, Calcd: 20.8% for **1**; Expt: 23.7%, Calcd: 22.8% for **2**; Expt: 19.5%, Calcd: 18.8% for **3**; Obsd: 19.9%, Calcd: 18.8% for **4**). Compounds **3** and **4** with rigid coligands exhibit slightly higher stability than **2** bearing flexible coligand.

3.6. Luminescent properties

The solid-state emission spectra of **1–4** were measured to explore potential applications as fluorescent materials (figure 6). Upon excitation at *ca* 360 nm, the four samples

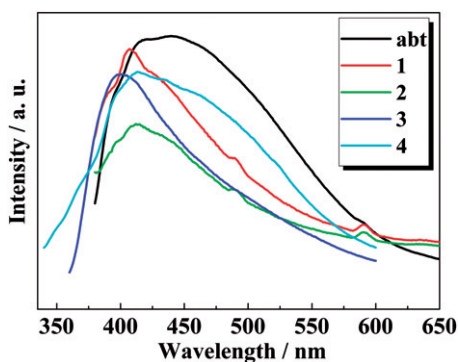


Figure 6. Solid-state emission spectra of **1–4** and free abt at room temperature.

display a maximum emission at 408 nm for **1**, 413 nm for both **2** and **4**, and 400 nm for **3**. Under comparable experimental conditions, a relatively broad emission at 440 nm could be observed for free abt resulting from the $\pi-\pi^*$ transition. In contrast, free H₂bd and H₂chdc are nearly non-fluorescent, and *o*-Hmb and *m*-Hmb display weak emissions at 360 nm upon excitation at 307 nm. Thus, comparable emissions for **1–4** can be assigned to the abt-based intraligand electron transfer, suggesting potential applications of the four complexes as luminescent materials. Compared with the isolated abt, the slightly modified intensity of the complexes may be attributed to increased rigidity of the complexes by ligand binding to the metal ion. The small shift of the emission suggests that the cation binding significantly perturbs the energy level of the π orbitals of abt.

4. Conclusion

Four abt-based Cd^{II} complexes were synthesized by the conventional room-temperature evaporation method. The structural diversity of these complexes is influenced by the number of carboxylate groups and skeleton flexibility of the coligand. The four complexes display favorable thermal stability and intense abt-based luminescent emissions, suggesting their potential applications as fluorescent materials.

Supplementary material

Crystallographic data (excluding structure factors) for the crystal structures reported in this article have been deposited with the Cambridge Crystallographic Data Center (CCDC Nos 847898–847901). This material can be obtained free of charge via www.ccdc.cam.ac.uk/conts/retrieving.html (or from the CCDC, 12 Union Road, Cambridge CB2 1EZ, UK; Fax: +44 1223 336033; E-mail: deposit@ccdc.cam.ac.uk).

Acknowledgments

This work was financially supported by the National Natural Science Foundation of China (20871092, 20973125, 21171129, and 21173157), the Program for New Century Excellent Talents in University (NCET-08-0914), which are gratefully acknowledged.

References

- [1] M. O'Keeffe, O.M. Yaghi. *Chem. Rev.*, **112**, 675 (2012).
- [2] (a) R. Sessoli, A.K. Powell. *Coord. Chem. Rev.*, **19**, 2328 (2009); (b) Z.H. Lu, J.X. Zhou, A.J. Wang, N. Wang, X.N. Yang. *J. Mater. Chem.*, **21**, 4161 (2011); (c) L.J. Murray, M. Dincă, J.R. Long. *Chem. Soc. Rev.*, **38**, 1294 (2009); (d) Y.-F. Zeng, X. Hu, F.-C. Liu, X.-H. Bu. *Chem. Soc. Rev.*, **38**, 469 (2009); (e) T.-L. Hu, J.-R. Li, C.-S. Liu, X.-S. Shi, J.-N. Zhou, X.-H. Bu, J. Ribas. *Inorg. Chem.*, **45**, 162 (2006); (f) Z. Huang, H.-B. Song, M. Du, S.-T. Chen, X.-H. Bu. *Inorg. Chem.*, **43**, 931 (2004).
- [3] (a) S.D. Bergman, D. Reshef, S. Groysman, I. Goldberg, M. Kol. *Chem. Commun.*, 2374 (2002); (b) M. Fourmigué, P. Batail. *Chem. Rev.*, **104**, 5379 (2004).
- [4] I. Hutchinson, S.A. Jennings, B.R. Vishnuvajjala, A.D. Westwell, M.F.G. Stevens. *J. Med. Chem.*, **45**, 744 (2002).
- [5] B.G. Chand, U.S. Ray, G. Mostafa, J. Cheng, T.H. Lu, C. Sinha. *Inorg. Chim. Acta*, **358**, 1927 (2005).
- [6] (a) E.-C. Wang, J. Li, Y.-L. Li, E.-C. Yang, X.-J. Zhao. *Synth. React. Inorg. Met.-Org. Nano-Met. Chem.*, **41**, 791 (2011); (b) Q. Chen, E.-C. Yang, R.-W. Zhang, X.-G. Wang, X.-J. Zhao. *J. Coord. Chem.*, **61**, 1951 (2008).
- [7] K. Davarskia, J. Macicekb, L. Konovalovc. *J. Coord. Chem.*, **38**, 123 (1996).
- [8] L. Sieron, M. Bukowska-Strzyzewska. *Acta Cryst.*, **C56**, 19 (2000).
- [9] E.-C. Yang, Y.-N. Chan, H. Liu, Z.-C. Wang, X.-J. Zhao. *Cryst. Growth Des.*, **9**, 4933 (2009).
- [10] (a) X.-G. Wang, J. Li, B. Ding, E.-C. Yang, X.-J. Zhao. *J. Mol. Struct.*, **876**, 268 (2008); (b) E.-C. Yang, H.-K. Zhao, B. Ding, X.-G. Wang, X.-J. Zhao. *New J. Chem.*, **31**, 1887 (2007).
- [11] G.M. Sheldrick. *SHELXS-97, Program for X-ray Crystal Structure Solution*, Göttingen University, Göttingen, Germany (1997).
- [12] G.M. Sheldrick. *SHELXL-97, Program for X-ray Crystal Structure Refinement*; Göttingen University, Göttingen, Germany (1997).
- [13] K. Nakamoto. *Infrared and Raman Spectra of Inorganic and Coordination Compounds*, 4th Edn, Wiley, New York (1986).